Science and Technology of Advanced Materials

ISSN: (Print) (Online) Journal homepage: https://www.tandfonline.com/loi/tsta20

Zn_2SnO_4 ternary metal oxide for ultraviolet radiation filter application: a comparative study with TiO_2 and ZnO

Kadhim Al-Attafi, Amar Al-Keisy, Muhammad A. Alsherbiny & Jung Ho Kim

To cite this article: Kadhim Al-Attafi, Amar Al-Keisy, Muhammad A. Alsherbiny & Jung Ho Kim (31 Oct 2023): Zn_2SnO_4 ternary metal oxide for ultraviolet radiation filter application: a comparative study with TiO_2 and ZnO, Science and Technology of Advanced Materials, DOI: 10.1080/14686996.2023.2277678

To link to this article: https://doi.org/10.1080/14686996.2023.2277678

Publisher: Taylor & Francis & The Author(s). Published by National Institute for Materials Science in partnership with Taylor & Francis Group.

Journal: *Science and Technology of Advanced Materials*

DOI: 10.1080/14686996.2023.2277678

Zn_2SnO_4 ternary metal oxide for ultraviolet radiation filter application: a comparative study with TiO_2 and ZnO

Kadhim Al-Attafi [1,2,*], Amar Al-Keisy [3] , Muhammad A. Alsherbiny [4,5], and Jung Ho Kim [1]

[1] Institute for Superconducting and Electronic Materials, Australian Institute for Innovative Materials (AIIM), University of Wollongong, North Wollongong, NSW 2500, Australia; kadhim@uow.edu.au (K.A-A.); jhk@uow.edu.au (J.H.K)

[2] Department of Physics, College of Science, University of Kerbala, Karbala 56001, Iraq; kadhim.m@uokerbala.edu.iq (K.A-A.)

[3] Nanotechnology and Advanced Material Research Center, University of Technology-Iraq, Baghdad 10066, Iraq; Amar.H.Alkeisy@uotechnology.edu.iq (A.A-K)

[4] Department of Pharmacognosy, Faculty of Pharmacy, Cairo University, Cairo 11562, Egypt; Muhammad.alshrbiny@pharma.cu.edu.eg (M.A.A)
[5] NICM Health Research Institute, Western Sydney University, Westmead, NSW 2145, Australia; Maz.Ali@westernsydney.edu.au (M.A.A)

* Corresponding author: Kadhim AL-ATTAFI

kadhim.m@uokerbala.edu.iq

Keywords: Zn_2SnO_4 ternary metal oxide, UV radiation filters, UVB and UVA blocking, TiO_2 and ZnO alternatives, TiO_2 free radicals, ZnO toxicity

Abstract

Ultraviolet (UV) radiation causes serious health risks to living organisms. Inorganic metal oxides, such as titanium dioxide (TiO_2) and zinc oxide (ZnO), have long been recognized for their effectiveness as UV radiation filters/blockers in sunscreen formulations. TiO_2 and ZnO as UV-blocking materials have some limitations and issues such as producing harmful radicals and toxicity, respectively. As a result, there is a growing need to develop efficient and safe UV-blocking materials to overcome these limitations associated with conventional

TiO_2 and ZnO materials. Zinc stannate (Zn_2SnO_4), a ternary metal oxide, is expected to be a promising candidate due to its optical properties and potential for UV-blocking capability. This manuscript presents a comprehensive investigation into the development and characterization of Zn_2SnO_4 as a potential alternative filter to TiO_2 and ZnO for UV protection. The fundamental characteristics, including structural, optical, and photocatalytic characteristics, as well as cell viability, were investigated for two Zn_2SnO_4 morphologies: cubic aggregate Zn_2SnO_4 nanoparticles (ZTO CANP) and Zn_2SnO_4 nanoparticles (ZTO NP), which were compared with the performance of TiO_2 nanoparticles (TiO_2 NP) and ZnO nanoparticles (ZnO NP). Interestingly, in addition to their promising UVB and partial UVA blocking properties, ZTO CANP and ZTO NP were found to be relativity photocatalytically inactive materials, which means they produce less free radical species as in the case of TiO_2 NP, and they are not considered as toxic materials as in the case of ZnO NP. To the best of our knowledge, this is the first direct comparison study examining the performance of Zn_2SnO_4 ternary metal oxide for its potential use as a UV filter. Further research and optimization need to be done on these materials, particularly ZTO CANP as a promising alternative UV filter.

1. Introduction

UV radiation has significant health risks, including skin damage, premature aging, and increased skin cancer. Nowadays, UV protection concerns have attracted the communities' research focus.[1-3] Sunlight contains three main wavelength ranges of ultraviolet (UV) radiation: UVA (320-400 nm), UVB (280-320 nm), and UVC (100-280 nm). UVC is the most harmful, but it is absorbed by the ozone layer. UVB is responsible for sunburns and erythema, causing skin redness and DNA damage, which leads to skin cancers. [4-6] Sunscreens based on organic /inorganic filters are widely utilized for skin UV protection. Using organic UV filters such as oxybenzone and octinoxate has concerns regarding their potential effects on the environment and potential risks to human health. [7] On the other hand, inorganic UV filters can reflect, scatter, and, depending on particle size, even absorb UV and visible light, forming a protective barrier on the skin. Examples of this category include iron oxide, red veterinary petrolatum, talc, calamine, kaolin, cerium dioxide, hydrotalcite, hydroxyapatite and cerium orthophosphate, zinc oxide (ZnO), and titanium dioxide (TiO_2). Among these, ZnO and TiO_2 are the most widely used and accepted inorganic

UV filters, as they are the only ones officially registered and approved as inorganic sunscreen ingredients.[8] These two filters are considered safe and relatively stable, showing no reactivity with organic filters. Nowadays, TiO_2 and ZnO are extensively utilized in sunscreens, cosmetics, and coatings due to their excellent UV absorption and scattering properties. [7] Nonetheless, the demand for more efficient, environmentally friendly, and cost-effective UV blockers is driving the investigation of novel materials. [8,9]

The inorganic UV filter materials should meet specific requirements, such as UV absorption efficiency, which is crucial in determining how well the material can block or absorb harmful UV radiation.[10] A wider band gap typically means more efficient UV absorption.[11] Inorganic sunscreen filters must show the capability to effectively shield UV radiation across the entire UVA/UVB spectrum (280-400 nm). [11,12] This is achieved through the absorption, scattering, and reflection properties of UV filters, which, in turn, are influenced by inherent refractive indices, particle sizes, dispersion within the emulsion base, and the thickness of the protective film. [12] ZnO and TiO_2 particle dimensions should be reduced to below 100 nm. Larger particles appear opaque due to reflection, while smaller particles have a sleek, translucent appearance.[13] Another factor is the photocatalytic activity of the UV filter material, for example, TiO_2 is known for its high photocatalytic activity, which can lead to the degradation of pollutants. For UV filters, however, this property might not be desired, as it could cause the breakdown of the filter itself and produce free radical species that harm the skin or the body cells. [14] TiO_2 is more capable than ZnO of triggering the creation of free radicals when subjected to UV radiation, which gives rise to worries about potential photo-mutagenesis. Studies suggest that TiO_2 nanoparticles have an even greater propensity to generate free radicals compared to their larger counterparts. [15] Furthermore, UV filters are desired to be transparent to visible light and not cause a whitened appearance. [16] Additionally, long-term stability, low cost, and biocompatibility (non-toxicity) of the materials are essential for practical applications. Although ZnO is widely used in various commercial products, including UV filters, it has a risk of toxicity when it penetrates body cells. [13,17] The higher photocatalytic activity of TiO_2 and the potential harmful toxicity of ZnO limit their use in sunscreen applications. Thus, there is a need to develop cost-effective, non-toxic, and photocatalytically inactive materials and evaluate their potential as alternative UV filters to TiO_2 and ZnO. [7,8]

The effectiveness of TiO_2 and ZnO and nanoparticles against UV exposure is related to their particle size. [8] ZnO exhibits consistent light absorption across both the UVA and the UVB ranges. In contrast, the absorption of TiO_2 is predominantly shifted toward the UVB spectrum when the particle size decreases. [18] UVB is responsible for inducing sunburn or UV-induced erythema, which is notably more severe than UVA.[19] To ensure comprehensive protection, a UVA protection factor needs to be at least one-third of the UVB protection factor. [10] Along with the undesired high photocatalytic activity of TiO_2, which affects the skin cells [8], the phototoxicity and the self-toxicity induced by ZnO have also raised concerns about the use of ZnO-based sunscreen ingredients. [20,21] The phototoxicity of ZnO depends on its photocatalytic activity (nanoparticle size) and surface reactivity which can be mitigated by modifying them, while the self-toxicity of ZnO is still limiting its use as an inorganic sunscreen filter. [21]

Based on the above, two main issues, which are the high photocatalytic activity of TiO_2 and the high toxicity of ZnO, need to be overcome by either combining them with other suitable materials or developing new inorganic filters. [8] Previously, we reported cubic Zn_2SnO_4 (aggregated nanoparticles) as a photoanode for dye-sensitized solar cells. This Zn_2SnO_4 showed higher photostability, which showed much lower organic dye degradation (organic D149) compared to TiO_2.[22] The low photocatalytic activity of Zn_2SnO_4 motivated us to conduct further investigation of the potential of using this material as a UV filter in comparison with TiO_2 and ZnO.

In general, the electronic structure of photocatalytic materials is primarily determined by their crystal structure, which plays a crucial role in influencing the overall photocatalytic performance. [23] As observed in previous studies, Kudo and Kato found that the photocatalytic activities of $BaTa_2O_6$ with different crystal phases, including tetragonal, hexagonal, and orthogonal structures, exhibit significant variations. Specifically, the orthogonal $BaTa_2O_6$ showed the highest photocatalytic activity while the hexagonal $BaTa_2O_6$ showed the lowest performance.[24] He et al. demonstrated that hexagonal $ZnIn_2S_4$ outperforms cubic $ZnIn_2S_4$. Fan et al. reported that monoclinic $BiVO_4$ exhibits superior photocatalytic performance compared to tetragonal $BiVO_4$. Barnes et.al reported that tetragonal TiO_2 showed higher photocatalytic activity than hexagonal ZnO.[25] based on these studies, It can be assumed that the order of crystalline phase structures based on their photocatalytic activity is (orthogonal, monoclinic, tetragonal, hexagonal, and cubic).

Herein, for obtaining a realistic comparison, two morphologies of Zn_2SnO_4, including nanoparticles (ZTO NP) and cubic aggregated nanoparticles (ZTO CANP), have been examined for their potential use as UV filter materials. This study includes a comparison with TiO_2 NP and ZnO NP, comprehensively exploring the performance of ZTO CANP and ZTO NP in terms of their UV filtering properties. The objective of this study was to assess the UV absorption effectiveness of ZTO relative to TiO_2 NP and ZnO NP. This evaluation includes band-gap energy, photocatalytic activity, transparency, and crystalline structures. Furthermore, the research will assess the toxicity of ZTO and its appropriateness as a UV filter.

2. Experimental methods

2.1 Nanomaterials synthesis

A series of inorganic metal oxides, ZTO CANP, ZTO NP, TiO_2 NP, and ZnO NP, were synthesized using the solvothermal method. The choice of precursors was based on previous reports in the literature. Briefly, to synthesize ZTO CANP, 1 mmol of zinc acetate dihydrate and 1 mmol of sodium stannate were dissolved in ethanol and water (1:1 v/v). The mixture was solvothermally heated to 180°C for 12 hours, and then centrifuged, dried, and calcinated at 400°C for 6 hours.[22] For ZTO NP, a modified solvothermal procedure was used to create a precursor solution. The process involved dissolving 0.15 M of zinc acetate dihydrate and 0.08 M of tin chloride pentahydrate in ethanol, stirring continuously for 2 hours, adding 0.5 M of sodium hydroxide, and subjecting the solution to solvothermal treatment at 180°C for 12 hours.[26] To prepare TiO_2 NP, 1.5 g of titanium isopropoxide (TTIP) was added into a solvent of ethanol and acetic acid (2:1 v/v), followed by stirring for 1 hour at ambient temperature. The solution was transferred to a Teflon-lined stainless-steel autoclave, heated to 200°C, and maintained at this temperature for 9 hours. The precipitate was collected, washed three times with distilled water and ethanol, dried overnight at 90°C, and then subjected to calcination at 500°C in an air environment for three hours. To prepare ZnO NP, a solution of zinc acetate dihydrate was prepared at a concentration of 0.1 M by dissolving it in 100 ml of distilled water. The solution was continuously stirred for 15 minutes with the application of heat as an assisting factor. The solution was solvothermally heated to 150°C for 9 hours, and then centrifuged, dried, and calcinated at 400°C for 3 hours.

2.2 Nanomaterial characterization techniques

The synthesized materials were characterized using several techniques, such as X-ray diffraction (XRD), transmission electron microscopy (TEM), and UV-visible (UV-Vis) spectroscopy, and the photocatalytic activity and cell viability were determined in terms of evaluating material toxicity. A GBC Scientific Equipment X-ray diffractometer was set at 30 mA, 40 kV, and employed to analyze the crystalline diffraction peaks of materials. The diffraction measurements were conducted using Cu Kα radiation with a wavelength of 1.54 Å. The scanning range was from 2θ = 20° to 80°, with a scan rate of 1° per minute. The morphology and internal structure of the materials were analyzed using transmission electron microscopy (TEM) with a JEOL JEM-2010 instrument. The optical measurements were performed with an ISR-3100 integrating sphere in conjunction with a UV-3600 Shimadzu spectrophotometer for films 3 µm in thickness deposited by a screen printer on quartz substrates. The film thickness measurements were conducted using a surface profiler (Veeco Dektak 150). The photocatalytic activities of materials were assessed for dye degradation using simulated sun illumination (Oriel LCS-100, 100 mW/cm^2). The Rhodamine B dye, with a concentration of 95% from Sigma, was evenly distributed in an aqueous solution. The catalyst loading was about 20 mg per 20 ml of a 25 µM dye solution.

2.3 Cell culturing process and cell viability experiments

MDAMB231 cells were sourced from the American Type Culture Collection (ATCC), specifically the NICM stock cells at the Western Sydney School of Medicine. These cells were cultivated in high-glucose Dulbecco’s modified Eagle’s medium (DMEM; 4.5 g/l glucose, Lonza, NSW, Australia). The culture medium was supplemented with 10% fetal bovine serum (obtained from Bio-Strategy PTY, Campbellfield, VIC 3061, Australia) and 1% penicillin-streptomycin solution (Sigma-Aldrich, Castle Hill, NSW, Australia). The cells were kept at a controlled temperature of 37°C in an atmosphere with a regulated CO_2

concentration of 5%. The cell maintenance procedures were conducted every 48–72 hours, allowing for the cells to form confluent monolayers.

To assess cell viability, the Alamar Blue assay, as described by Ahmed, Gogal Jr, et al. in 1994, [27] was employed. In 96-well plates, cells were cultured with a seeding density of 105 cells/mL in 100 µL. After 24 hours, the cells were exposed to the test samples, which were dissolved in dimethyl sulfoxide (DMSO). This incubation period lasted for 72 hours. As part of the experimental design, doxorubicin was utilized as a positive control at a concentration of 1 µM, with 0.1% DMSO serving as the negative control for each plate. Upon completion of the incubation period, the culture media were removed, and 100 µL of a 0.1 mg/mL Alamar Blue solution (resazurin) was added to each well. The Alamar Blue solution was prepared as a stock solution (1 mg/mL) in freshly prepared phosphate-buffered saline (PBS) and subsequently diluted 1:10 with a medium that lacked fetal bovine serum (FBS). The absorbance was then measured at wavelengths of 570 nm and 600 nm using a BMG LABTech FLUOstar OPTIMA plate reader located in Mount Eliza, Victoria, Australia. The tests were conducted three times, and negative control was introduced to denote full cell viability (100%).

3. Results and discussions

3.1 Structure characterizations

The XRD patterns in Figure 1a-d reveal that all the synthesized metal oxides exhibit single-phase crystalline structures without any other phase impurities. Figure 1a-b indicated that both ZTO CANP and ZTO NP exhibit the characteristic cubic spinel structure (JCPDS no. 00–24–1470). The XRD analysis in Figure 1c confirms the tetragonal crystalline structure of anatase phase TiO_2 NP (JCPDS no. 21–1272). Figure 1d confirms the hexagonal crystalline structure of ZnO NP (JCPDS no. 36–1451). The crystalline structure types of ZNO CANP and ZTO NP are different than those of TiO2 NP and ZnO NP which can significantly affect their photoelectronic properties and thus their photocatalytic activities. [23,28] (This will be discussed in detail in the 3.3 section)

The TEM images in Figure 2a-c, along with the accompanying particle size distributions in the insets, offer a comprehensive understanding of the particles' characteristics. In Figure 2a, the ZTO CANP structure showcases cubic nanostructures formed through the aggregation of nanoparticles. These aggregates exhibit an average particle size of 75±15 nm.

Additionally, the individual nanoparticles within this structure are found to be approximately 5.0±1.5 nm in size. Figure 2b validates the particle size of ZTO NP to be around 8±2 nm. For comparative purposes, Figure 2c and Figure 2d present the particle sizes of TiO_2 NP and ZnO NP, measured as approximately 16±4 nm and 22±5 nm, respectively. Collectively, the TEM analysis established that all the examined materials possess nanoparticle size within the nanoscale range, specifically measuring below 100 nm. This nanoscale dimension renders these materials highly promising for applications as UV-blocking filters.

3.2 Optical characterizations

The UV-Vis spectra in Figure 3a-d demonstrate the optical properties of the synthesized materials, highlighting their potential use as UV filters. Figure 3a-d compares their optical properties, including transmittance, reflectance, absorption, and absorption coefficients as well as the optical band gaps for UV-blocking purposes. As shown in Figure 3a, ZTO CANP and ZTO NP demonstrated good UV-blocking properties; particularly in the UVB range as well as partially blocking UVA. TiO_2 can primarily block UVB wavelengths and partially block UVA, while ZnO can block both UVA and UVB ranges due to its broad UV-blocking capability. It is well known that reflectance depends on the refractive index of the material and its surface properties. [29] Generally, all such materials tend to have relatively low reflectance in the UV region due to their semiconducting nature.[30] From Figure 3b, both ZTO CANP and ZTO NP showed the highest reflectance over the whole wavelength range (200-800 nm). This means that ZTO can reflect much higher UV, visible, and near-infrared (NIR) light compared to TiO_2 and ZnO. Interestingly, ZTO CANP and ZTO NP have two reflection regions in UVAI (320-400 nm), which show 10-16% and 18-21% reflection, respectively, while TiO_2 NP and ZnO NP have only one reflection region, which is located at 360 nm (3%) and 390 (12%), respectively. As can be seen, TiO_2 NP has lower reflection due to its high transparency, while despite ZTO NP and ZnO NP being nanoparticles, they showed high reflectance compared to TiO_2 NP due to their aggregation. ZTO CANP showed the highest reflectance due to the faceted nature of its cubic structure. It is worth mentioning that both ZTO materials represent a combination of the reflectance capabilities of TiO_2 NP and ZnO NP.

As shown in Figure 3c, ZTO CANP and ZTO NP have absorption bands in the UV region, contributing to their UV-blocking properties. Their absorption spectra are nearly identical and represent the average absorption of TiO_2 NP and ZnO NP. This indicates broader UVA range absorption than TiO_2 NP and slightly lower than ZnO. TiO_2 NP, however, has absorption bands in the UVB region. They absorb UVB wavelengths effectively, while, ZnO NP has strong absorption in both the UVB and the UVA regions, making these nanoparticles efficient UV blockers. Unfortunately, the inherent toxicity and phototoxicity of ZnO NP limits its potential to be used as a UV filter.

The absorption coefficient indicates how strongly a material absorbs light. Higher values indicate stronger absorption. As shown in Figure 3c, ZTO CANP and ZTO NP showed lower absorption coefficients in the UV region, contributing to their UV-blocking capabilities, particularly for UVB. TiO_2 NP has a high absorption coefficient in the UVB range, which makes it suitable for UVB protection. ZnO NP has a relatively high absorption coefficient in both the UVB and UVA ranges, making it effective for broad-spectrum UV protection.

Figure 4a-c shows the band-gap measurements of the materials determined through Tauc plots, where all the materials have very close similarity in their band gaps located in the UV range (375.8-387.5 nm), corresponding to the band-gap range of (3.3-3.2 eV). This indicates that all the materials can absorb UV radiation and serve as UV filters. As known, the crystal structure phase influences the band gap, the separation, and transport efficiencies of photogenerated carriers in photocatalysts.[28,30] It can be noted that all materials have a close value of band gap which indicates similar absorption over the UV region.

3.3 Photocatalytic characterizations of materials

Figure 5a and b shows the photocatalytic measurements of ZTO CANP, ZTO NP, TiO_2 NP, and ZnO In terms of Rhodamine B dye degradation under simulated sunlight. As indicated in Figures 5a and b, showing the dye concentration degradation and the degradation constant (K), respectively, TiO_2 NP caused the highest dye degradation rate, while ZTO CANP caused the lowest degradation. ZTO NP and ZnO showed slightly higher dye degradation than ZTO CANP. It can be concluded that TiO_2 NP can be considered a highly active photocatalytic material (~30% degradation rate during 1 hour) which implies that high free radical species are produced due to the higher charge separation. On the other hand. ZTO CANP, ZTO NP, and ZnO can be considered inactive photocatalytic materials (~2%, ~7 %, and ~7%, respectively), which means that they are expected to produce much lower free radical species than TiO_2 NP. These findings confirm the high photoactivity of TiO_2 NP and the low photoactivity of ZnO NP, which are well consistent with what was reported previously. [15] The higher activity of TiO_2 NP can be attributed to the high absorption coefficient of TiO_2, as shown in Figure 3d. One of the important requirements for UV filter materials is to be photocatalytically inactive to avoid producing harmful free radicals that can cause skin aging, burning, and cancer. Therefore, ZTO CANP and ZTO NP have similar UV performance to TiO_2, however, they are expected to produce lower free radicals making them more suitable for use as UV filters in terms of satisfying this condition. ZnO is well known, however, as a high inherent toxicity and photo-toxicity material, which limits its use as a UV filter. [13,17]

The difference in dye degradation findings can be further interpreted for more understanding. Photocatalytic activity is related to three main factors: light absorption, charge carrier transfer and separation, and surface reactions. these factors determine the efficiency of solar-to-chemical energy conversion within pristane semiconductors. [31] As shown in Figure 4, all materials have close values of band gaps in the range of (3.2-3.3 eV) suggesting that the difference in their light absorption efficiencies is not the primary reason for the difference in their photocatalytic activities. Additionally, the XRD traces in Figure 1 indicate that all materials exhibited well crystallinity, however, they have different crystalline systems. It can be concluded that the cubic spinel crystalline structure of ZTO CANP and ZTO NP and the hexagonal structure of ZnO NP are more likely to show lower photocatalytic activities while the tetragonal structure of TiO_2 NP is likely to show higher photocatalytic activity. [23]

Since the morphology of the catalyst can impact the number of active sites.[32] From Figure 2, ZTO NP, TiO_2 NP, and ZnO NP have nanoparticulate structures with particle sizes (8, 16, and 22 nm respectively). While, ZTO CANP has facets cubic aggregated nanoparticles with a size of 75 nm for the cubic structure and 5 nm for the individual aggregated nanoparticles, which may affect the surface active sites and thus cause the lowest photocatalytic activity. .[28] Thus, the morphology in terms of the particle size and surface area has a minor effect and is likely not the predominant factor affecting their photocatalytic activity as there is no significant difference between their particle sizes. Based on this, assuming that ZTO CANP, ZTO NP, and ZnO NP materials can generate more holes and electrons, it is plausible that they do not effectively reach the surface, emphasizing the significance of carrier dynamics as a potential key factor contributing to the differing activities between them and TiO_2 NP.

Recently, It has been reported that the electron-hole diffusion length length plays a significant role in determining the photocatalytic activity.[28] The highest photocatalytic activity of TiO_2 NP mainly rises from high diffusion length correlated with low electron-hole recombination due to the indirect band gap of TiO_2 NP (Figure 4c) which allows less recombination. [23,33] The other materials have direct band gaps which are more likely to allow more electron-hole recombination. Despite, ZNO NP has been reported as having a high diffusion length,[34] the higher charge recombination correlated with its direct band gap affecting the photocatalytic activity.[23,33] As the diffusion length of photogenerated electron-hole is a function of their corresponding lifetime, our previous study confirmed that TiO_2 NP has a higher diffusion length than ZTO CANP and ZTO NP.[22]

To conclude, The lowest diffusion length of electron-hole which hinders them from being transferred to the surface along with the high recombination rate are the most significant factors affecting the number of active sites that make ZTO CANP inactively photo-catalyzed.

3.4 Toxicity characterizations of materials

ZnO has been reported as an anti-breast-cancer agent due to its reducing cell viability as well as an antibacterial agent. [35,36] We used the available breast cancer cells (MDAMB231) to evaluate the cell viability against the self-toxicity of the materials as a toxicity test. MDAMB231 cells can be used to test the toxicity of nanomaterials by evaluating cell viability. It is a commonly used human breast cancer cell line in the research on and toxicity testing of nanomaterials. To investigate the inherent or self-toxicity of the ZTO CANP, ZTO NP, TiO_2 NP, and ZnO NP, cell viability measurements were conducted *in vitro* using MDAMB231 cells in the presence of different concentrations of the materials to evaluate their inherent toxicities in a dark condition. The results of the cell viability assays were analyzed to determine the effects of the nanomaterials on the MDAMB231 cells. A decrease in cell viability compared to the untreated control cells could indicate the toxicity level. As shown in Figures 6a and b, ZnO showed very low cell viability (approximately zero at 50-200 µg/ml concentrations), while, ZTO CANP, ZTO NP, and TiO_2 NP showed approximately the same higher cell viability, which was about 95% compared to ZnO NP. ZTO CANP and ZTO NP were found to again satisfy another important requirement (the same as TiO_2), which is lower inherent toxicity. Interestingly, even though ZTO NP has a very small particle size, which could easily penetrate the skin, it showed approximately 100% cell viability. It can be concluded that ZTO CANP and ZTO NP could be more suitable materials to use as UV filters, particularly in the UVB region, due to their low toxicity and low production of free radicals. As is well known, the high number of free radicals produced by TiO_2 is undesirable for its use as a UV filter and needs to be suppressed by suitable approaches. It is important to note that the toxicity observed in these tests might not directly translate to real-world scenarios, because *in-vitro* cell culture models might not fully capture the complexities of *in-vivo* systems. Nevertheless, cell viability assays using cell lines such as MDAMB231 can provide valuable preliminary data on the potentially toxic effects of nanomaterials, at least as a lower or first estimation indicator.

4. Conclusions

This study highlights the development of two morphologies of Zn_2SnO_4 (ZTO) inorganic ternary metal oxides as promising alternatives to TiO_2 NP and ZnO NP for UV radiation protection. Their unique crystal structures, optical properties, and potential variations in band-gap energy, as well as their expected low photocatalytic activity and toxicity, make these materials attractive candidates for further investigation. These findings showed that both ZTO CANP and ZTO NP exhibit similar promising UVB blocking and partial UVA blocking to TiO_2 NP. They can be considered identical combinations of the UV-blocking profiles of TiO_2 NP and ZnO NP. Interestingly they showed much lower photocatalytic activities, which can lead to much lower production of free radicals than for TiO_2 NP. Additionally, ZTO CANP and ZTO NP showed very low inherent toxicity compared to ZNO NP. Once again, they can overcome the toxicity limitation associated with ZnO NP. The findings of this comparative study would help researchers and industry understand the potential of Zn_2SnO_4, typically ZTO CANP as a UV radiation filter and its advantages over the commonly used TiO_2 NP and ZnO NP. This may pave the way for the development of more efficient and cost-effective UV filters with a focus on environmental and health benefits. Following this study, further discussions, characterization, and analysis will be conducted to examine the performance of

ZTO CANP and ZTO NP materials as composites with either TiO_2 NP or ZnO NP in terms of UV blocking, photocatalytic activity, and inherent toxicity.

Future research should enhance synthesis techniques, evaluate stability, assess phototoxicity, and explore practical applications of novel inorganic ternary metal oxides for UV radiation protection materials.

Author contributions

All authors organized and agreed on the research content.

Funding: This research was funded by the Australian Research Council and the National Research Foundation of Korea (NRF), as well as the Higher Committee for Education Development in Iraq (HCED) and the Ministry of Higher Education and Scientific Research, University of Kerbala, Iraq.

Acknowledgments: The authors acknowledge the Australian Institute for Innovative Materials (AIIM) at the University of Wollongong, Australia, for granting them equipment access. They also acknowledge the Higher Committee for Education Development (HCED) and the Ministry of Higher Education & Scientific Research, University of Kerbala, Iraq, for their financial assistance.

Conflicts of interest: The authors state that they have no competing interests.

References

[1] Chavda VP, Acharya D, Hala V, et al. Sunscreens: A comprehensive review with the application of nanotechnology. Journal of Drug Delivery Science and Technology. 2023 2023/09/01/;86:104720.

[2] Badry R, El-Nahass MM, Nada N, et al. Structural and UV-blocking properties of carboxymethyl cellulose sodium/CuO nanocomposite films. Scientific Reports. 2023 2023/01/20;13(1):1123.

[3] Nitulescu G, Lupuliasa D, Adam-Dima I, et al. Ultraviolet Filters for Cosmetic Applications. Cosmetics. 2023;10(4):101.

[4] Guan LL, Lim HW, Mohammad TF. Sunscreens and Photoaging: A Review of Current Literature. American journal of clinical dermatology. 2021 Nov;22(6):819-828.

[5] Young AR, Claveau J, Rossi AB. Ultraviolet radiation and the skin: Photobiology and sunscreen photoprotection. Journal of the American Academy of Dermatology. 2017 Mar;76(3s1):S100-s109.

[6] Miyamura Y, Coelho SG, Wolber R, et al. Regulation of human skin pigmentation and responses to ultraviolet radiation. Pigment cell research. 2007 Feb;20(1):2-13.

[7] Schneider SL, Lim HW. A review of inorganic UV filters zinc oxide and titanium dioxide. Photodermatology, photoimmunology & photomedicine. 2019 Nov;35(6):442-446.

[8] Nery É M, Martinez RM, Velasco MVR, et al. A short review of alternative ingredients and technologies of inorganic UV filters. Journal of cosmetic dermatology. 2021 Apr;20(4):1061-1065.

[9] Seixas VC, Serra OA. Stability of sunscreens containing $CePO_4$: proposal for a new inorganic UV filter. Molecules (Basel, Switzerland). 2014 Jul 9;19(7):9907-25.

[10] Jiménez Reinosa J, Leret P, Álvarez-Docio CM, et al. Enhancement of UV absorption behavior in ZnO–TiO_2 composites. Boletín de la Sociedad Española de Cerámica y Vidrio. 2016 2016/03/01/;55(2):55-62.

[11] Serpone N, Dondi D, Albini A. Inorganic and organic UV filters: Their role and efficacy in sunscreens and suncare products. Inorganica Chimica Acta. 2007 2007/02/15/;360(3):794-802.

[12] Schneider SL, Lim HW. A review of inorganic UV filters zinc oxide and titanium dioxide. Photodermatology, photoimmunology & photomedicine. 2019;35(6):442-446.

[13] Smijs TG, Pavel S. Titanium dioxide and zinc oxide nanoparticles in sunscreens: focus on their safety and effectiveness. Nanotechnology, science and applications. 2011 Oct 13;4:95-112.

[14] Picatonotto T, Vione D, Carlotti M, et al. Photocatalytic Activity of Inorganic Sunscreens. Journal of Dispersion Science and Technology - J DISPER SCI TECH. 2001 05/31;22:381-386.

[15] Osmond-McLeod M, McCall M. Zinc oxide nanoparticles in modern sunscreens: An analysis of potential exposure and hazard. Nanotoxicology. 2010 03/01;4:15-41.

[16] Forestier S. Rationale for sunscreen development. Journal of the American Academy of Dermatology. 2008 May;58(5 Suppl 2):S133-8.

[17] Osmond MJ, McCall MJ. Zinc oxide nanoparticles in modern sunscreens: An analysis of potential exposure and hazard. Nanotoxicology. 2010 2010/03/01;4(1):15-41.

[18] Beasley DG, Meyer TA. Characterization of the UVA protection provided by avobenzone, zinc oxide, and titanium dioxide in broad-spectrum sunscreen products. American journal of clinical dermatology. 2010 Dec 1;11(6):413-21.

[19] de Gruijl FR, Sterenborg HJ, Forbes PD, et al. Wavelength dependence of skin cancer induction by ultraviolet irradiation of albino hairless mice. Cancer research. 1993 Jan 1;53(1):53-60.

[20] George S, Yin H, Liu Z, et al. Hazard profiling of a combinatorial library of zinc oxide nanoparticles: Ameliorating light and dark toxicity through surface passivation. Journal of hazardous materials. 2022 Jul 15;434:128825.

[21] Ma H, Williams PL, Diamond SA. Ecotoxicity of manufactured ZnO nanoparticles – A review. Environmental Pollution. 2013 2013/01/01/;172:76-85.

[22] Al-Attafi K, Jawdat FH, Qutaish H, et al. Cubic aggregates of Zn_2SnO_4 nanoparticles and their application in dye-sensitized solar cells. Nano Energy. 2019 2019/03/01/;57:202-213.

[23] Bai S, Gao C, Low J, et al. Crystal phase engineering on photocatalytic materials for energy and environmental applications. Nano Research. 2019 2019/09/01;12(9):2031-2054.

[24] Kato H, Kudo A. Photocatalytic water splitting into H_2 and O_2 over various tantalate photocatalysts. Catalysis Today. 2003 2003/02/28/;78(1):561-569.

[25] Barnes RJ, Molina R, Xu J, et al. Comparison of TiO_2 and ZnO nanoparticles for photocatalytic degradation of methylene blue and the correlated inactivation of gram-positive and gram-negative bacteria. Journal of Nanoparticle Research. 2013 2013/01/22;15(2):1432.

[26] Burke A, Ito S, Snaith H, et al. The Function of a TiO_2 Compact Layer in Dye-Sensitized Solar Cells Incorporating “Planar” Organic Dyes. Nano Letters. 2008 2008/04/01;8(4):977-981.

[27] Longhin EM, El Yamani N, Rundén-Pran E, et al. The alamar blue assay in the context of safety testing of nanomaterials [Methods]. Frontiers in Toxicology. 2022 2022-September-28;4.

[28] He Y, Liu Y, Li C, et al. Origin of the Photocatalytic Activity of Crystalline Phase Structures. ACS Applied Energy Materials. 2022 2022/07/25;5(7):8923-8929.

[29] Piri N, Shams-Nateri A, Mokhtari J. The relationship between refractive index and optical properties of absorbing nanoparticle. Color Research & Application. 2016;41(5):477-483.

[30] Shree S, Paradisanos I, Marie X, et al. Guide to optical spectroscopy of layered semiconductors. Nature Reviews Physics. 2021 2021/01/01;3(1):39-54.

[31] Bai S, Jiang J, Zhang Q, et al. Steering charge kinetics in photocatalysis: intersection of materials syntheses, characterization techniques and theoretical simulations [10.1039/C5CS00064E]. Chemical Society Reviews. 2015;44(10):2893-2939.

[32] Tong H, Ouyang S, Bi Y, et al. Nano-photocatalytic materials: possibilities and challenges. Advanced materials (Deerfield Beach, Fla). 2012 Jan 10;24(2):229-51.

[33] Luttrell T, Halpegamage S, Tao J, et al. Why is anatase a better photocatalyst than rutile? - Model studies on epitaxial TiO_2 films. Scientific Reports. 2014 2014/02/10;4(1):4043.

[34] Kumar RR, Kumar KU, Haranath D. 9 - Synthesis, characterization, and applications of ZnO–TiO2 nanocomposites. In: Pawade VB, Dhoble SJ, Swart HC, editors. Nanoscale Compound Semiconductors and their Optoelectronics Applications: Woodhead Publishing; 2022. p. 271-314.

[35] Pouresmaeil V, Haghighi S, Raeisalsadati AS, et al. The anti-breast cancer effects of green-synthesized zinc oxide nanoparticles using carob extracts. Anti-Cancer Agents in Medicinal Chemistry (Formerly Current Medicinal Chemistry-Anti-Cancer Agents). 2021;21(3):316-326.

[36] Sivakumar P, Lee M, Kim Y-S, et al. Photo-triggered antibacterial and anticancer activities of zinc oxide nanoparticles [10.1039/C8TB00948A]. Journal of Materials Chemistry B. 2018;6(30):4852-4871.

Figure 1: X-ray diffraction patterns of (a) ZTO CANP, (b) ZTO NP, (c) TiO_2 NP, and (d) ZnO NP.

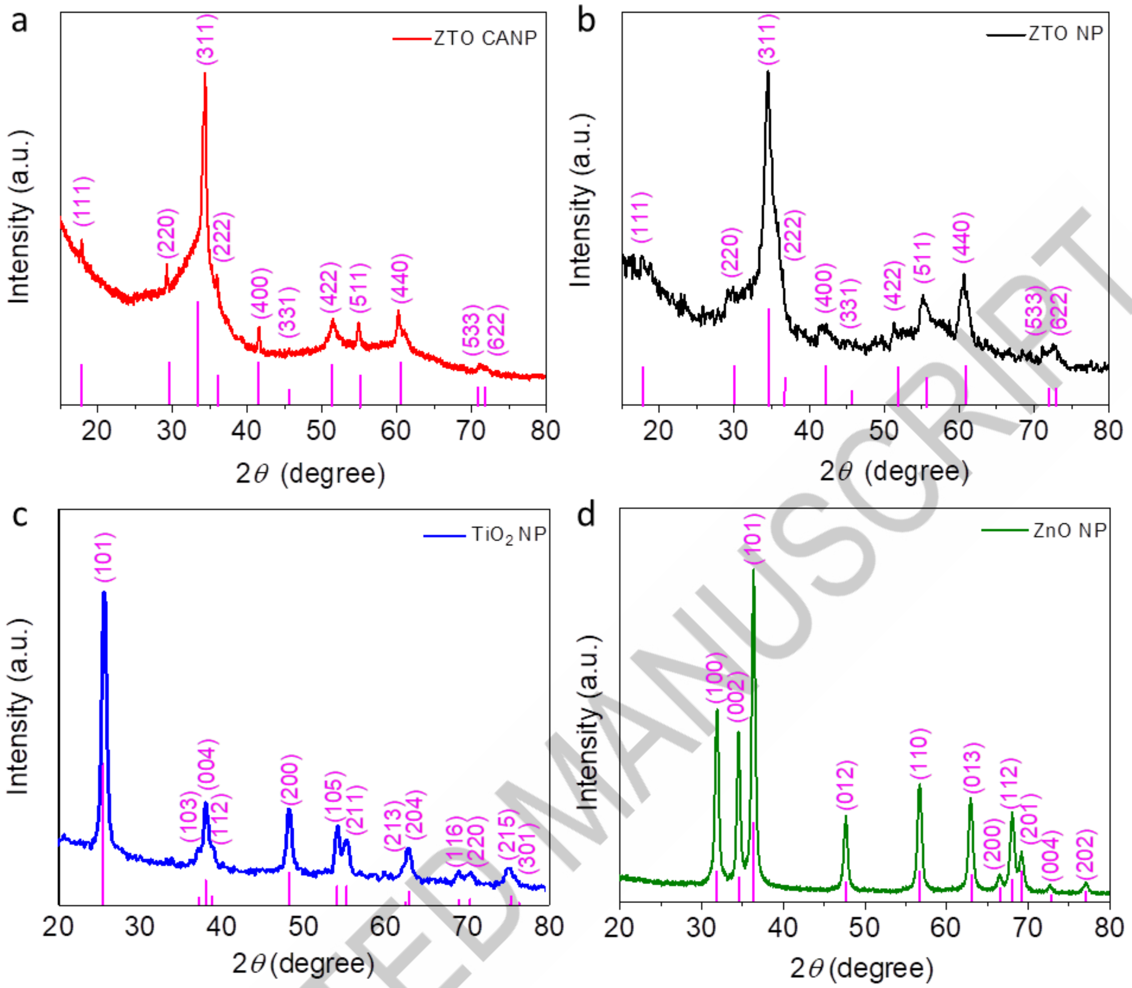

Figure 2: TEM images with the insets showing the particle size distributions of (a) ZTO CANP, (b) ZTO NP, (c) TiO_2 NP, and (d) ZnO NP.

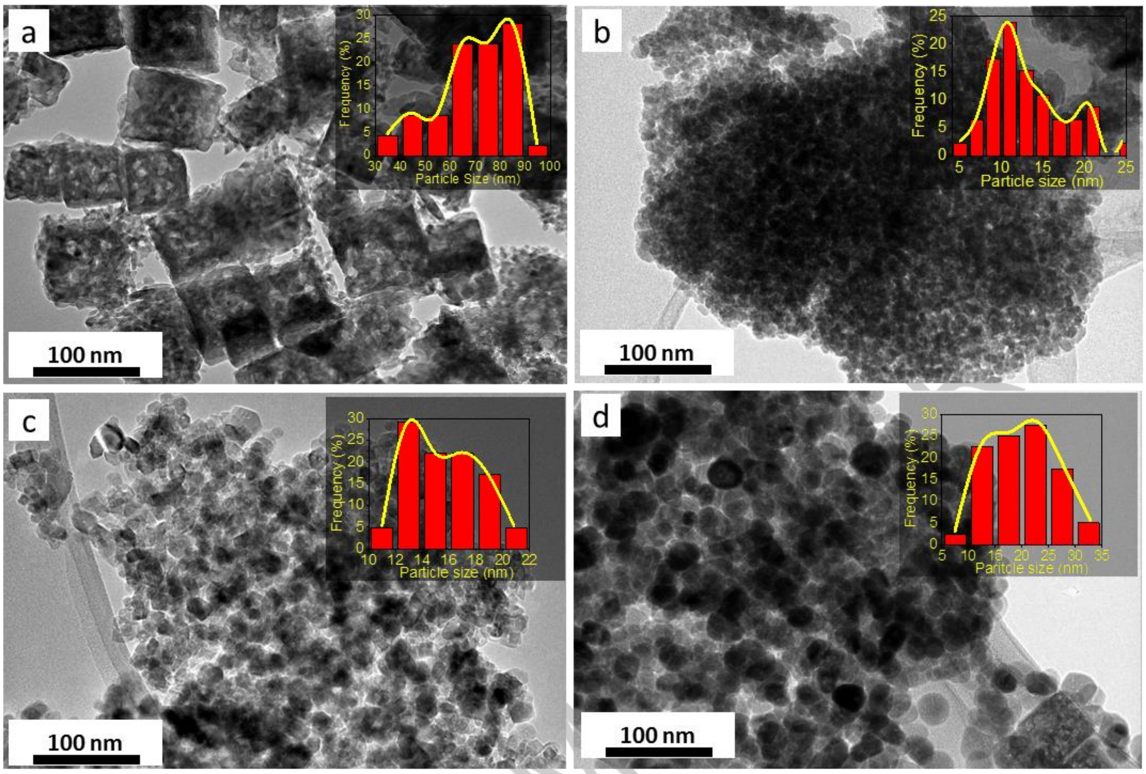

Figure 3: Optical parameters: (a) transmittance, (b) reflectance, (c) absorbance, and (d) absorption coefficient spectra of ZTO CANP, ZTO NP, TiO_2 NP, and ZnO NP.

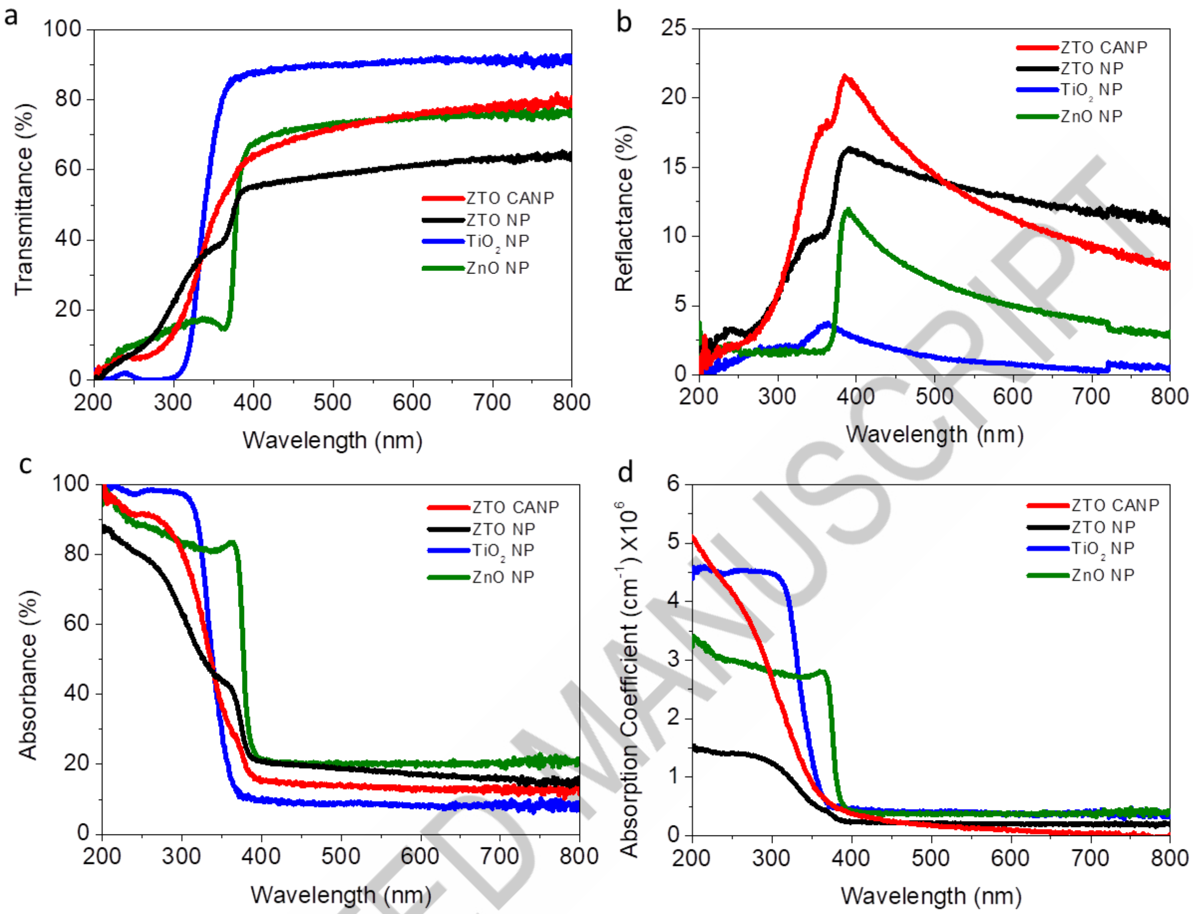

Figure 4: Optical energy band-gap measurements (Tauc plots) of (a) ZTO CANP, (b) ZTO NP, (c) TiO_2 NP, and (d) ZnO NP.

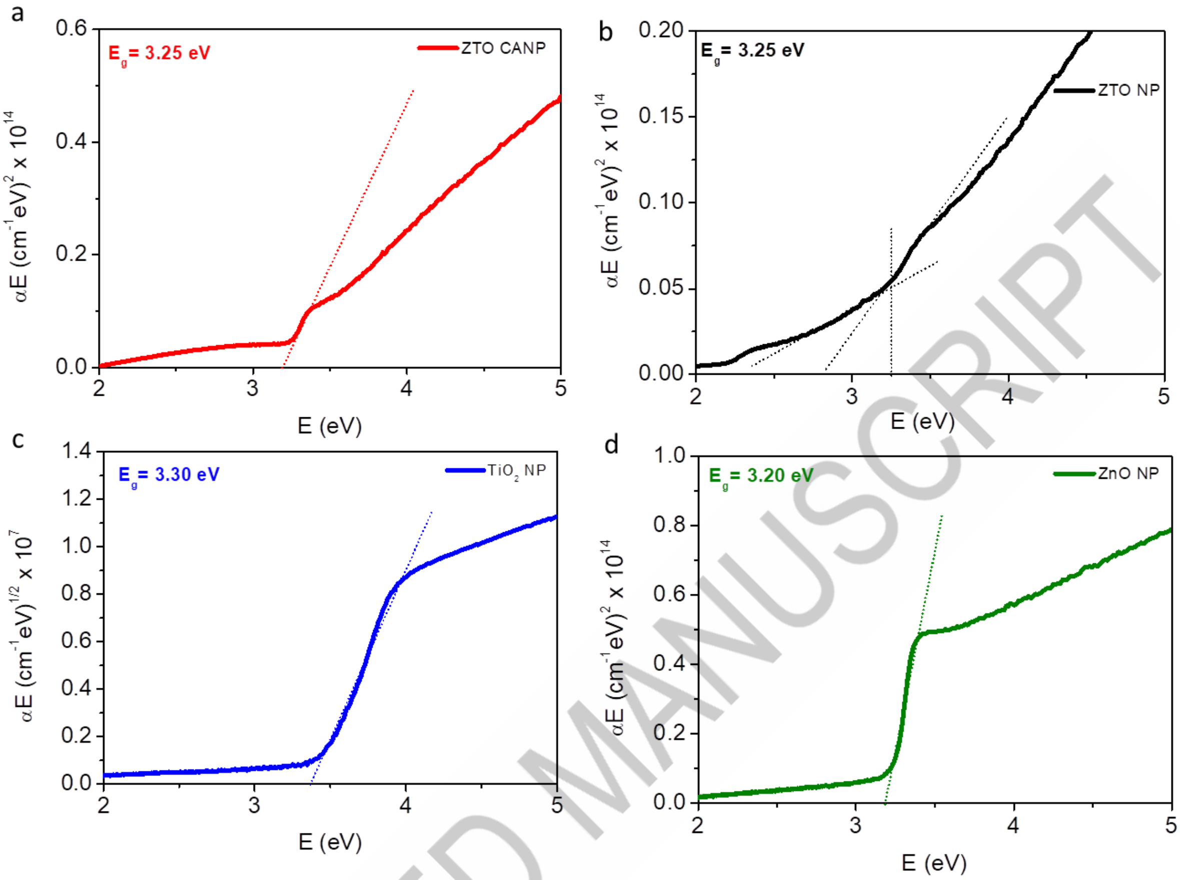

Figure 5: Photocatalytic measurements: (a) Rhodamine B dye degradation and (b) Rhodamine B dye degradation constants (K) of ZTO CANP, ZTO NP, TiO_2 NP, and ZnO NP.

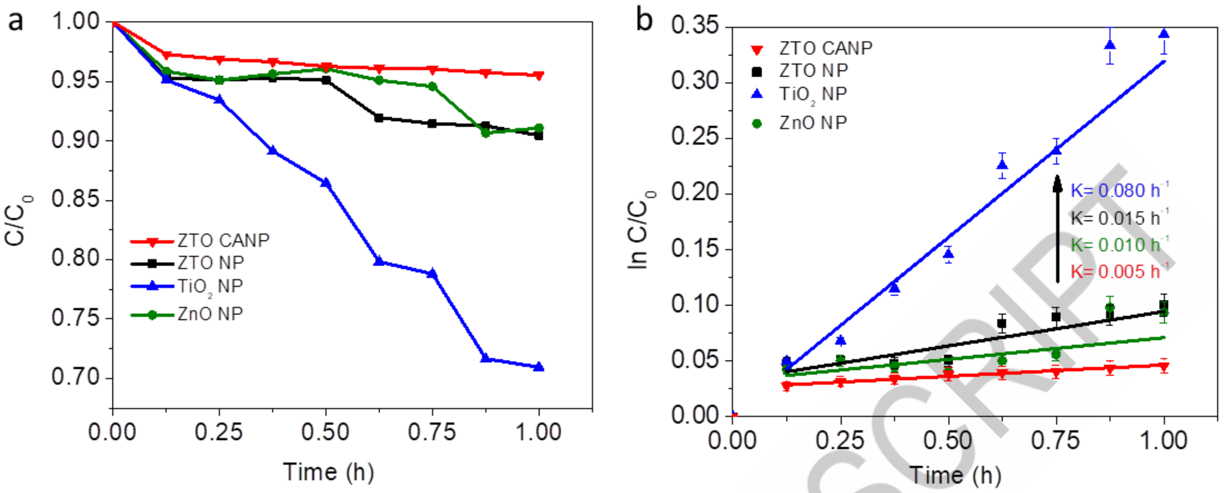

Figure 6: (a) and (b) *In-vitro* toxicity analysis of ZTO CANP, ZTO NP, TiO_2 NP, and ZnO NP at different concentrations in the dark.

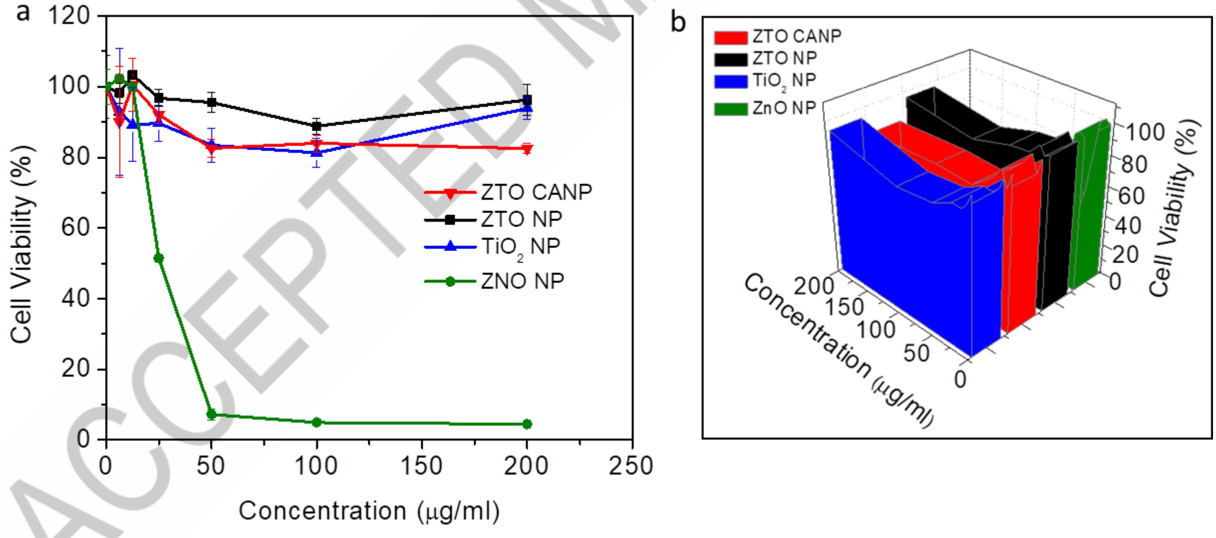

Zn_2SnO_4 vs. TiO_2 & ZnO

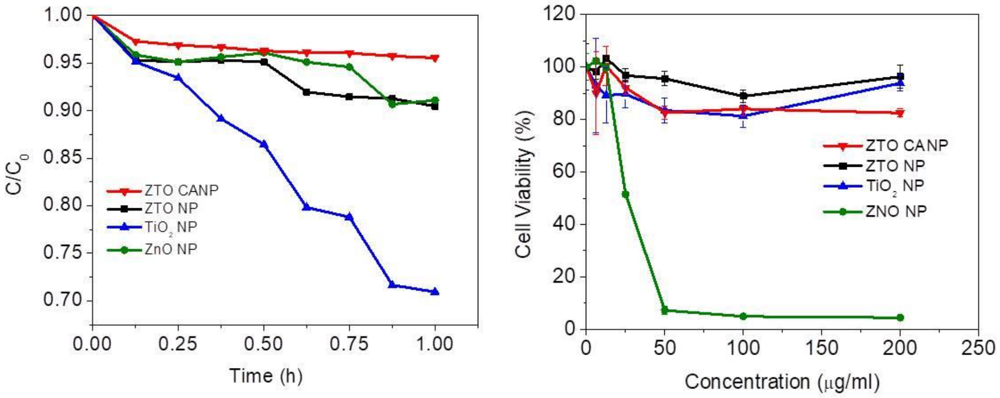

Much Lower free radicals & toxicity

Graphical Abstract

Novelty statement

This study investigates the development and characterization of zinc stannate (Zn2SnO4) as a potential alternative UV-blocking material for sunscreen formulations. Despite their effectiveness as UV radiation filters, TiO2 and ZnO have harmful radicals and toxicity, respectively. The study focuses on two Zn2SnO4 morphologies: cubic aggregate Zn2SnO4 nanoparticles (ZTO CANP) and Zn2SnO4 nanoparticles (ZTO NP). They showed promising UVB and partial UVA blocking. Their UV blocking range seems to be an average of the blocking profile of TiO2 and ZnO .ZTO CANP and ZTO NP are found to be photocatalytically inactive, producing less free radical species and not being toxic. To the best of our knowledge, this is the first direct comparison study examining the performance of Zn2SnO4 ternary metal oxide for its potential use as a UV filter.